YMTHE, Volume *30*

Supplemental Information

Limited astrocyte-to-neuron conversion in the mouse brain using NeuroD1 overexpression

David Leib, Yong Hong Chen, Alex Mas Monteys, and Beverly L. Davidson

Supplemental figure

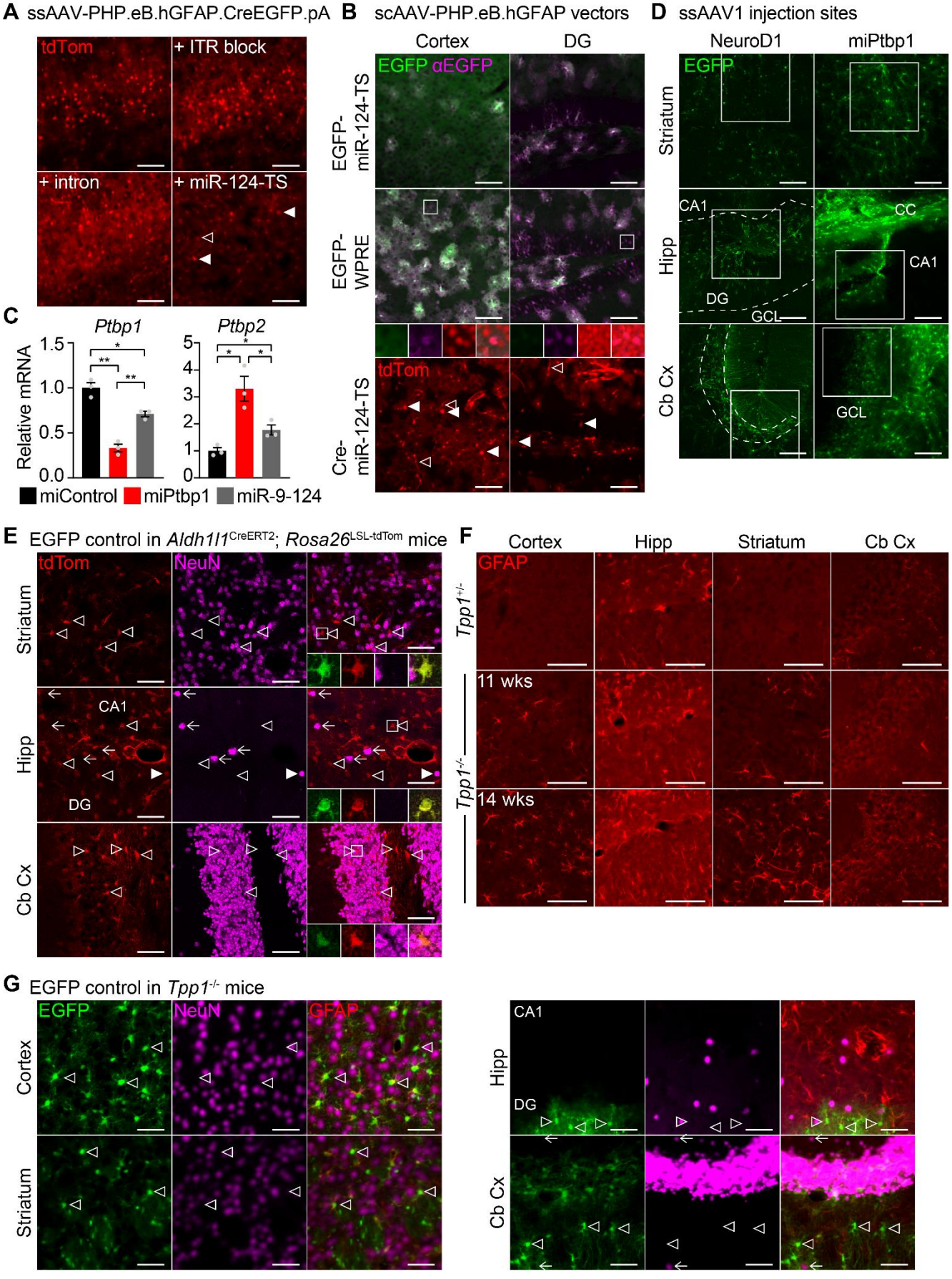

Figure S1: Supporting data

(A) tdTom fluorescence images from cerebral cortex of *Rosa26*$^{LSL\text{-}tdTom}$ mice (n=3-4) injected retro-orbitally with 1E11 vg of ssAAV-PHP-eB.hGFAP.CreEGFP.pA vectors. An inverted terminal repeat (ITR) transcription block (top right), synthetic intron (bottom left), and 3' UTR miR-124 targeting site (miR-124-TS; bottom right) were added sequentially to the original vector (top left). The ITR block had no effect, the intron increased the number of tdTom+ cells, and the miR-124-TS helped restrict tdTom expression to astrocytes, though some sparse Cre recombination still occurred in neurons (solid arrowheads) and endothelial cells (open arrowhead). No EGFP fluorescence was detected (data not shown). Scale bars, 100 µm. (B) Fluorescence images from C57BL6/J or *Rosa26*$^{LSL\text{-}tdTom}$ mice (n=2) injected retro-orbitally with scAAV-PHP-eB.hGFAP vectors. scAAV-PHP-eB.hGFAP.EGFP.miR-124-TS (3.16E11 vg; top row) transduced glia across the CNS, shown as merged EGFP direct fluorescence (green) and immunofluorescence (magenta). Replacing the miR-124-TS with a WPRE increased EGFP fluorescence despite a lower dose (1.0E11 vg; longer fluorescence exposure in top row than 2nd row). However, the WPRE vector led to low-level expression in neurons that co-stained for EGFP (magenta) and NeuN (red, insets) in the cortex and DG. scAAV-PHP-eB.hGFAP.Cre.miR-124-TS transduced glia across the CNS, but also NeuN-positive neurons (solid arrowheads) and endothelial cells (open arrowheads). Results were similar in other areas of the central nervous system, including striatum and cerebellar cortex (data not shown). Scale bars, 100 µm. (C) RT-qPCR data from Neuro-2a cells showing knockdown of *Ptbp1* and downstream upregulation of *Ptbp2* by miR-9-124 and miPtbp1 compared to miControl (n=3 biological repeats). One-way repeated-measure ANOVAs were significant for both genes (*Ptbp1*, $F=384.4$, $p=0.0008$; *Ptbp2*, $F=39.86$, $p=0.0224$), and Holm-Šídák multiple comparisons were performed (*, $p<0.05$, **, $p<0.01$). Data represent mean±SE. (D) Low-magnification confocal images showing viral EGFP expression for NeuroD1 conversion experiments (Figure 1E, 1F) and fluorescence images showing viral EGFP expression for miPtbp1 conversion experiments (Figure 1G). Regions with astrocyte-to-neuron conversion in NeuroD1-treated hippocampus and cerebellum are outlined with dashed lines. Boxed regions are included in Figures 1E and 1G. Scale bars, 100 µm. (E) Immunofluorescence from mice (n=2) injected with an EGFP control for the NeuroD1 conversion experiment in *Aldh1l1*^{CreERT2}; *Rosa26*$^{LSL\text{-}tdTom}$ mice (Figure 1E). Open arrowheads, transduced tdTom+ cells that do not co-localized with NeuN. Insets show EGFP expression (green) for a representative cell. Solid arrowhead, single tdTom+ cell that co-localized with NeuN but did not express EGFP from the AAV. Arrows, neurons with no tdTom or EGFP expression. Scale bars, 50 µm. (F) Gfap immunostaining confirming progressive astrogliosis in Tpp1$^{-/-}$ mice at 11 (n=2) and 14 weeks (n=7) of age. Images from 14-week-old mice were taken from the contralateral side of the brains in Figure 1I but displayed with brighter contrast settings. Scale bars, 100 µm. (G) Immunofluorescence from mice injected with an EGFP control (n=1) for NeuroD1 conversion in Tpp1$^{-/-}$ mice (Figure 1I). Open arrowheads, EGFP+ cells that do not co-localize with NeuN. Arrows, NeuN+ neurons that do not co-localized with EGFP. Scale bars, 50 µm. ITR, inverted terminal repeat; DG, dentate gyrus; Hipp, hippocampus; Cb cx, cerebellar cortex; GCL, granule cell layer.

Supplemental methods

Animals

Animal protocols were approved by The Children's Hospital of Philadelphia Institutional Animal Care and Use Committee. Mice were housed in a controlled temperature and humidity environment on a 12-hour light/dark cycle according to the Guide for the Care and Use of Laboratories animal. Food and water were provided ad libitum. C57BL/6J, *Aldh1l1*^{CreERT2}, and *Rosa26*$^{LSL\text{-}tdTom}$ mice were obtained from The Jackson Laboratory (JAX #000664, #031008, and #007914) and maintained in house. Tpp1$^{-/-}$ males were crossed with Tpp1$^{+/-}$ females in house to generate Tpp1$^{-/-}$ mice.

Design and *in vitro* testing of miPtbp1

An artificial microRNA targeting mouse *Ptbp1* (miPtbp1) based on a previously published shRNA (target sequence: 5'-CTCAATGTCAAGTACAACAAT-3')[1] was embedded in a microRNA backbone similar to human miR-30.[2] For *in vitro* experiments, miPtbp1 or two control microRNAs were cloned downstream of a U6 promoter. As a positive control, the combined mouse microRNAs miR-9 and -124 were used (miR-9-124), since miR-124 targets *Ptbp1*[3] and miR-9-124 has been previously shown to convert fibroblasts to neurons *in vitro*.[4] As a negative control, a previously described microRNA[5] was included.

Ptbp1 knockdown by miPtbp1 was confirmed in Neuro-2a cells. In three independent experiments, cells were seeded at 75,000 cells per well in 24-well plates and transfected with 500 ng of plasmid DNA using Lipofectamine 3000 (Invitrogen). After 48 hours, cells were rinsed once with PBS and RNA collected using Trizol (Invitrogen). cDNA was generated using MultiScribe reverse transcriptase (Invitrogen) and random priming. qPCR was then performed on a Bio-Rad CFX384 machine using TaqMan Universal Master Mix II (Applied Biosystems) and the following primer/probe mixes (ThermoFisher): *Ptbp1* (Mm01731480_gH), *Ptbp2* (Mm00497922_m1), and *Gapdh* (Mm99999915_g1). Gene expression was calculated relative to *Gapdh* and normalized to non-transfected controls within each experiment, and the combined data from multiple experiments was normalized to miSafe control. Statistical analysis was performed in Graphpad Prism 9.2.0.

Virus production

AAV shuttle plasmids were constructed with AAV2 inverted terminal repeats (ITRs) for single-stranded AAVs (ssAAVs) or modified ITRs to produce self-complementary AAVs (scAAVs),[6] the human GFAP ABC_1D promoter (hGFAP),[7] and a 6.9-kb plasmid backbone to reduce cross-packaging. Mouse *Neurod1* cDNA followed by P2A-EGFP or EGFP alone were cloned downstream of the hGFAP promoter, and miPtbp1 or miControl were cloned into the 3'UTR of EGFP. A block sequence to stop transcription from the left ITR, a synthetic intron (Addgene plasmid #99129),[8] and four tandem miR-124 targeting sequences (miR-124-TS)[9] were cloned into the specified plasmids. Plasmid sequences were confirmed by Sanger sequencing (Genewiz), and ITR integrity was confirmed by SmaI restriction digest. AAVs were produced in house by triple transfection of HEK293 cells and purification by iodixanol ultracentrifugation. The following viruses were produced:

ssAAV-PHP.eB.hGFAP.CreEGFP.SV40pA

ssAAV-PHP.eB.block.hGFAP.CreEGFP.SV40pA
ssAAV-PHP.eB.block.hGFAP.intron.CreEGFP.SV40pA
ssAAV-PHP.eB.block.hGFAP.intron.CreEGFP.miR-124-TS.SV40pA
scAAV-PHP.eB.hGFAP.intron.EGFP.miR-124-TS.SV40pA
scAAV-PHP.eB.hGFAP.intron.EGFP.WPRE.SV40pA
scAAV-PHP.eB.hGFAP.intron.Cre.miR-124-TS.SV40pA
ssAAV1.block.hGFAP.intron.NeuroD1.2A.EGFP.miR-124-TS.SV40pA
ssAAV1.block.hGFAP.intron.EGFP.miR-124-TS.SV40pA
ssAAV1.block.hGFAP.intron.EGFP.miPtbp1.SV40pA
ssAAV1.block.hGFAP.intron.EGFP.miControl.SV40pA

AAV genome titers were determined by digital droplet PCR.

Virus infusions

AAV-PHP.eB viruses were injected retro-orbitally in a volume of 100 µl. Mice were 5-10 months old for scAAV experiments in C57BL6/J and *Rosa26*$^{LSL\text{-}tdTom}$ mice (Figure 1B, 1C, S1B), and 3-4 months old for ssAAV experiments in *Rosa26*$^{LSL\text{-}tdTom}$ mice (Figure S1A).

AAV1 viruses were delivered by stereotaxic injection as previously described[10] with the following coordinates:

Cerebral cortex: +0.86 mm rostral to bregma, +1.8 mm from midline, 1.7 mm deep
Striatum: +0.86 mm rostral to bregma, 1.8 mm from midline, 3.5 mm deep
Hippocampus: 1.7 mm caudal to bregma, 1.5 mm from midline, 2.0 mm deep
Cerebellum: 1.7 mm caudal to bregma, 1.5 mm from midline, 2.0 mm deep

For NeuroD1 and miPtbp1 conversion experiments in *Aldh1l1*^{CreERT2}; *Rosa26*$^{LSL\text{-}tdTom}$ mice, mice were pre-administered tamoxifen at 75 mg/kg for five consecutive days four weeks prior to surgery. For NeuroD1 conversion experiments (Figure 1E), mice were 10-15 months old at the time of infusion. For miPtbp1 conversion experiments (Figure 1G), mice were 4-10 months old. One miPtbp1-injected mouse died following surgery. Ten-week-old Tpp1$^{-/-}$ mice were injected with ssAAV1 vectors expression NeuroD1, EGFP, miPtbp1, and miControl (n=3). At this age, Tpp1$^{-/-}$ mice are sensitive to handling, and two mice injected with EGFP, two injected with miPtbp1, and one injected with miSafe died between surgery and euthanasia.

Tissue processing, immunofluorescence, and microscopy

Mice were transcardially perfused with ice-cold PBS and 4% paraformaldehyde. Brains were post-fixed overnight and cryoprotected in 30% sucrose before sectioning at a thickness of 40 µm on a freezing microtome. For immunofluorescence, floating sections were blocked in 5% goat serum in PBS with 0.1% triton (PBS-T) at room temperature for two hours, then incubated with primary antibodies at 4ºC overnight. The following day, sections were washed four times with PBS-T, then incubated with Alexa Fluor secondary antibodies (Invitrogen) in block buffer for one hour at room temperature, washed three times, incubated with Hoechst dye (Invitrogen) for five minutes, and rinsed. Stained sections were mounted on slides and coverslipped with Fluoro-Gel (Electron Microscopy Sciences). Images were acquired on a

Leica DM6000B microscope equipped with a 10X HC PLAPO (numerical aperture (NA) 0.4) lens and a Hammatsu Orca flash 4.0 monochrome camera, or a Leica SP8 confocal microscope equipped with a 40X HC PLAPO CS2 (NA 0.75) lens and HyD photodetectors. Images were processed in ImageJ. The following primary antibodies were used: NeuN (rabbit monoclonal, dilution 1:2000, Abcam ab177487), GFAP (mouse monoclonal, dilution 1:2000, SIGMA G 3893), EGFP (chicken polyclonal, dilution 1:500, Aves GFP-1020).

Supplemental references

1. Xue, Y., Ouyang, K., Huang, J., Zhou, Y., Ouyang, H., Li, H., Wang, G., Wu, Q., Wei, C., Bi, Y., Jiang, L., et al. (2013). Direct conversion of fibroblasts to neurons by reprogramming PTB-regulated microRNA circuits. Cell *152*, 82-96. 10.1016/j.cell.2012.11.045.
2. McBride, J.L., Boudreau, R.L., Harper, S.Q., Staber, P.D., Monteys, A.M., Martins, I., Gilmore, B.L., Burstein, H., Peluso, R.W., Polisky, B., Carter, B.J., et al. (2008). Artificial miRNAs mitigate shRNA-mediated toxicity in the brain: implications for the therapeutic development of RNAi. Proc Natl Acad Sci U S A *105*, 5868-5873. 10.1073/pnas.0801775105.
3. Makeyev, E.V., Zhang, J., Carrasco, M.A., and Maniatis, T. (2007). The MicroRNA miR-124 promotes neuronal differentiation by triggering brain-specific alternative pre-mRNA splicing. Mol Cell *27*, 435-448. 10.1016/j.molcel.2007.07.015.
4. Yoo, A.S., Sun, A.X., Li, L., Shcheglovitov, A., Portmann, T., Li, Y., Lee-Messer, C., Dolmetsch, R.E., Tsien, R.W., and Crabtree, G.R. (2011). MicroRNA-mediated conversion of human fibroblasts to neurons. Nature *476*, 228-231. 10.1038/nature10323.
5. McBride, J.L., Pitzer, M.R., Boudreau, R.L., Dufour, B., Hobbs, T., Ojeda, S.R., and Davidson, B.L. (2011). Preclinical safety of RNAi-mediated HTT suppression in the rhesus macaque as a potential therapy for Huntington's disease. Mol Ther *19*, 2152-2162. 10.1038/mt.2011.219.
6. McCarty, D.M., Fu, H., Monahan, P.E., Toulson, C.E., Naik, P., and Samulski, R.J. (2003). Adeno-associated virus terminal repeat (TR) mutant generates self-complementary vectors to overcome the rate-limiting step to transduction in vivo. Gene Ther *10*, 2112-2118. 10.1038/sj.gt.3302134.
7. Lee, Y., Messing, A., Su, M., and Brenner, M. (2008). GFAP promoter elements required for region-specific and astrocyte-specific expression. Glia *56*, 481-493. 10.1002/glia.20622.
8. Chan, K.Y., Jang, M.J., Yoo, B.B., Greenbaum, A., Ravi, N., Wu, W.L., Sanchez-Guardado, L., Lois, C., Mazmanian, S.K., Deverman, B.E., and Gradinaru, V. (2017). Engineered AAVs for efficient noninvasive gene delivery to the central and peripheral nervous systems. Nat Neurosci *20*, 1172-1179. 10.1038/nn.4593.
9. Taschenberger, G., Tereshchenko, J., and Kugler, S. (2017). A MicroRNA124 Target Sequence Restores Astrocyte Specificity of gfaABC1D-Driven Transgene Expression in AAV-Mediated Gene Transfer. Mol Ther Nucleic Acids *8*, 13-25. 10.1016/j.omtn.2017.03.009.
10. Keiser, M.S., Chen, Y.H., and Davidson, B.L. (2018). Techniques for Intracranial Stereotaxic Injections of Adeno-Associated Viral Vectors in Adult Mice. Curr Protoc Mouse Biol *8*, e57. 10.1002/cpmo.57.